Physical and stoichiometric controls on stream respiration in a headwater stream

Jancoba Dorley[1], Joel Singley[2,3], Tim Covino[4,5], Kamini Singha[6], Michael Gooseff[7,8], David Van Horn[9], Ricardo González-Pinzón[1]

Correspondence to: Ricardo González-Pinzón (gonzaric@unm.edu)

[1]Civil, Construction and Environmental Engineering, University of New Mexico, Albuquerque, NM USA
[2]Environmental Studies Program, University of Colorado, Boulder, CO USA
[3]Biology, Marine Biology, and Environmental Science, Roger Williams University, Bristol, RI USA
[4]Ecosystem Science and Sustainability, Colorado State University, Fort Collins, CO USA
[5]Department of Land Resources and Environmental Sciences, Montana State University, Bozeman, MT USA
[6]Geology and Geological Engineering, Hydrologic Science and Engineering Program, Colorado School of Mines, Golden, CO USA
[7]Civil, Environmental and Architectural Engineering, University of Colorado, Boulder, CO USA
[8]Institute of Arctic and Alpine Research, University of Colorado, Boulder, CO USA
[9]Department of Biology, University of New Mexico, Albuquerque, NM USA

Abstract. Many studies in ecohydrology focusing on hydrologic transport argue that longer residence times across a stream ecosystem should consistently result in higher biological uptake of carbon, nutrients, and oxygen. This consideration does not incorporate the potential for biologically mediated reactions to be limited by stoichiometric imbalances. Based on the relevance and co-dependences between hydrologic exchange, stoichiometry, and biological uptake, and acknowledging the limited amount of field studies available to determine their net effects on the retention and export of resources, we quantified how microbial respiration is controlled by the interactions and supply of essential nutrients (C, N, P) in a headwater stream in Colorado, USA. For this, we conducted two rounds of nutrient experiments, each consisting of four sets of continuous injections of Cl- as a conservative tracer, resazurin as a proxy for aerobic respiration, and one of the following nutrient treatments: a) N, b) N+C, c) N+P, and d) C+N+P. Nutrient treatments were considered as known system modifications to alter metabolism, and statistical tests helped identify the relationships between reach-scale hydrologic transport and respiration metrics. We found that as discharge changed significantly between rounds and across stoichiometric treatments, a) transient storage mainly occurred in pools lateral to the main channel and was proportional to discharge, and b) microbial respiration remained similar between rounds and across stoichiometric treatments. Our results contradict the notion that hydrologic transport alone is a dominant control on biogeochemical processing and suggest that complex interactions between hydrology, resource supply, and biological community function are responsible for driving in-stream respiration.

1 Introduction

High biochemical processing rates in streams and rivers occur at locations and times where the dynamic interconnections among hydrologic exchange, residence time, nutrient supply, and microbial biomass combine to form optimum conditions for metabolic activity (i.e., the transformation of nutrients, carbon, and oxygen or another electron acceptor into energy and biomass). The exchange of water between the main channel and transient storage zones, where most microbes exist, is the primary mechanism supplying carbon, nutrients, and oxygen to metabolically active zones (Gooseff et al. 2004; Covino et al. 2010b, 2011; Knapp et al. 2017; Gootman et al. 2020). The extent of water exchange controls the residence time of solutes (Drummond et al., 2012; Gomez et al., 2012; Patil et al., 2013), their chemical signatures (Covino and McGlynn 2007), as well as the microbial composition and their metabolic functioning (Blume et al. 2002; Navel et al. 2011; Li et al. 2020). Exchange patterns are influenced by geomorphologic conditions (Kasahara and Wondzell 2003; Cardenas et al. 2004; Gooseff et al. 2005; Emanuelson et al. 2022), hydrologic conditions (i.e., discharge and surrounding water table configuration) (Gooseff et al. 2005; Wondzell 2006; Ward et al. 2013; Ward and Packman 2019), and biofilm growth (Battin et al. 2003; Wen and Li 2018). The spatiotemporal variability in exchange processes and resource availability (e.g., seasonal variations in nutrient loads) create heterogeneous hydrologic and biogeochemical gradients across space and time, within which ecosystem metabolism occurs (Mulholland et al., 1985; Mulholland & Hill, 1997).

To date, studies with a focus on hydrologic transport argue that longer residence times across a stream ecosystem should consistently result in higher biological demand for carbon, nutrients, and oxygen (Valett et al. 1996; Gooseff et al. 2005; Wondzell 2006; Gomez et al. 2012; Zarnetske et al. 2012; Ward et al. 2013; Li et al. 2021), not fully incorporating the potential for biologically mediated reactions to be limited by stoichiometric imbalances. Ecological stoichiometry is the notion that biota balance the consumption of nutrients with energy requirements. Redfield (1934) noted that marine phytoplankton generally contained a ratio of C:N:P of 106:16:1 in their biomass, and these ratios are similar to those available in their environment. This "Redfield ratio" suggests that an ecosystem requires an optimal ratio of available nutrients to flourish and has been used as a guide for many other environmental stoichiometry studies. In a study of streams across eight biomes, Dodds et al. (2004) noted that N consumption depends in part on the C:N ratio of organic matter in streams and suggested that shifts in these state ratios likely influence N retention.

The net effect of supply and demand of resources can be explored at the reach scale with the non-dimensional Damköhler number, Da (Harvey et al. 2013; Pinay et al. 2015; Krause et al. 2017; Ocampo et al. 2020), which quantifies the ratio of transport (i.e., supply) to biological uptake (i.e., demand) timescales along flow paths (Oldham et al. 2013; Liu et al. 2022). Similar to any other non-dimensional number, Da offers simplicity and objectivity for inter-site and intra-site comparisons. Da has been used to provide insight into the factors limiting the supply and demand of resources (Harvey et al. 2005), as values of $Da \sim 1$ define a balance between transport and uptake time scales, which theoretically result in maximal resource retention. Accordingly, where or when $Da \ll 1$, i.e., the uptake timescale is much greater than the transport timescale, uptake is suboptimal, and it is referred to as reaction limited because even though resources became available through hydrologic exchange, they were not fully

73 taken up (i.e., assimilated). Conversely, where or when $Da >> 1$, i.e., the transport timescale is much greater than the

74 uptake timescale, resources become scarce or transport-limited, and biologically inactive subregions start to develop

75 (González-Pinzón and Haggerty 2013; Harvey et al. 2013; Gootman et al. 2020). While Da captures essential

76 components of the potential interactions between the supply and demand of ecologically relevant resources, it does

77 not explicitly capture the role of stoichiometric limitations on the supply (i.e., C:N:P ratios in water fluxes) and

78 demand (C:N:P biomass composition and needs) of resources (Tromboni et al. 2018). This is because Da numbers

79 are estimated from solute-specific mass balances, which inform transport and reaction timescales for one resource at

80 a time (e.g., only N), in isolation of other stoichiometrically relevant resources that can become limiting factors

81 (e.g., C and P).

82 Based on the relevance and co-dependences between hydrologic exchange, stoichiometry, and biological

83 uptake, and the limited amount of field studies available to determine their net effects on the retention and export of

84 resources, we sought to quantify how metabolic activity is controlled by the interactions and supply of essential

85 nutrients (C, N, P) at the reach scale. More specifically, we tested if variations in stoichiometric conditions can

86 induce metabolic limitations at which residence time alone becomes a weak predictor of stream respiration. We

87 addressed the following research question: *How is microbial respiration controlled by hydrologic exchange vs.*

88 *stoichiometric conditions (i.e., supply of C, N, and P)*? We hypothesized that aerobic respiration would be

89 maximized when nutrient supply and demand were nearly balanced for a given hydrologic condition. To test this, we

90 conducted a repeated set of stream tracer injections in Como Creek, a mountain stream in Colorado, USA, varying

91 stream C (acetate; sensu Baker et al., 1999), N ($NaNO_3$), and P (KH_2PO_4) concentrations to manipulate

92 stoichiometry and nutrient supply. We repeated experiments under different flow conditions to quantify the tradeoffs

93 between supply (transport and delivery of nutrients), and demand (microbial respiration). We tested for statistical

94 relationships between hydrologic transport metrics and respiration metrics using the resazurin-resorufin tracer

95 system (González-Pinzón et al., 2012; Knapp et al., 2018) and contextualized our findings within the framework of

96 the Damköhler number.

97 **2 Methods**

98 **2.1 Site Description**

99 Our research experiments were conducted in Como Creek, a forested pool and riffle stream in Colorado,

100 USA. Como Creek is a tributary to Boulder Creek, with land cover consisting of approximately 20% alpine

101 meadow-tundra and 80% conifer forest. The study reach drains a 5.4 km^2 catchment, with elevations ranging from

102 2895-3557 m and a mean average precipitation of 883 mm/y (Ries III et al. 2017; Emanuelson et al. 2022). Como

103 Creek has a snowmelt-driven hydrograph with stream discharges ranging from 1-98 L/s and features short-lived

104 increases in discharge during the monsoon season between July and August (Figure 1). The study reach is a multi-

105 thread channel with substrate ranging from small gravel to bedrock. Additionally, the channel has an average width-

106 to-depth ratio of 11.5, a sinuosity of 1.1, and an average longitudinal slope of 21% (Natural Resources Conservation

107 Service).

108
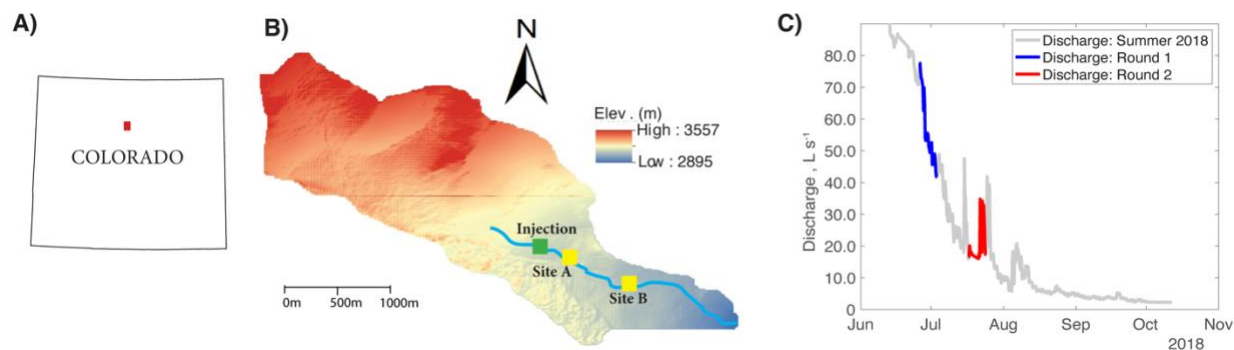
109
110 **Figure 1: A) Location of Como Creek watershed in Colorado, B) detailed map of the watershed where Sites A and B are**
111 **50 and 350 m downstream from the injection location, and C) hydrograph and timing of experimental work; each round**
112 **of experiments consisted of four treatments featuring N, N+C, N+P, and C+N+P nutrient additions.**
113

114 **2.2 Stream tracer injection experiments**

115   We conducted two rounds of experiments, each consisting of four sets of continuous injections (lasting ~ 4-
116 7 h) of Cl^- as a conservative tracer, resazurin (referred to as Raz hereafter) as a proxy for aerobic respiration, and one
117 of the following nutrient treatments: a) N, b) N+C, c) N+P, and d) C+N+P. In our study, the nutrient treatments are
118 treated as known system modifications (control variables) to alter metabolism. Also, we use the transformation of
119 Raz, which occurred at the same spatiotemporal scales of the nutrient additions, to calculate how changes in
120 stoichiometric conditions and discharge affect respiration. Briefly, the reactive tracer Raz (blue in color) is
121 irreversibly reduced to resorufin (Rru, red) under aerobic respiration, and the relationship between Raz
122 transformation and oxygen consumption is linear (González-Pinzón et al. 2012, 2014, 2016; Knapp et al. 2018;
123 Dallan et al. 2020).

124   Before each tracer injection, we used the Tracer Injection Planning Tool (TIPT) (González-Pinzón et al.
125 2022) to estimate the amount of tracer mass needed to reach steady state conditions at the downstream site and to
126 estimate the duration of the tracer breakthrough curves. From our field sampling, ambient concentrations of nitrate
127 averaged 0.035 (±0.002) mg/L. We corroborated this value with a study by (Smith et al. 2003), who generated
128 estimates of background total nitrogen (TN) and total phosphorous (TP) yield and concentrations throughout the
129 stream-river network in 14 ecoregions of the conterminous US. That study found 75th % quartile TN= 0.21 (±0.05)
130 mg/L and TP= 0.02 (±0.005), which indicates relatively low nutrient concentrations compared to agricultural
131 streams in the US Midwest featuring ambient concentrations of up to two orders of magnitude higher. Based on
132 estimated discharges and reach lengths, we targeted a maximum concentration of 2 mg/L for Cl, and 100 μg/L at the
133 most downstream locations. The concentrations for nitrogen, phosphorus, and carbon were based on the expected
134 detection limit of phosphate (i.e., 0.1 mg/L) for common ion chromatographs. From that minimum phosphate
135 concentration expected, we scaled the masses of nitrogen and carbon using the 106C:16N:1P Redfield ratio
136 (Redfield, 1934). Table 1 shows the masses injected and the discharges observed during the studies. Note that we
137 allowed the stream to return to ambient concentrations for one day after each set of injections.
138

139
140

Table 1: Tracer injection data for each round of experiments at Como Creek.

Date	Treatment	Discharge (L/s)	Start time	End time	NaCl (g)	KNO₃ (g)	KPO₄ (g)	Sodium Acetate (g)	Raz (g)
Round 1									
6/26/18	N	74	11:30	17:00	32653	502	-	-	150
6/28/18	N+C	61	10:08	14:10	32680	500	-	2000	150
6/30/18	N+P	53	10:00	17:00	32680	500	400	-	150
7/2/18	C+N+P	49	9:59	14:00	32680	500	400	2000	150
Round 2									
7/17/18	N	20	10:30	14:35	10000	100	-	-	30
7/19/18	N+C	17	10:00	13:59	10000	100	-	400	30
7/21/18	N+P	17	10:00	14:06	10000	100	80	-	30
7/23/18	C+N+P	25	9:30	13:35	10000	100	80	400	30

141
142 We collected 20 mL aliquots in each tracer injection 50m and 350m downstream of the injection site
143 (labeled Sites A and B, Figure 1) to generate tracer breakthrough curves (BTCs) for Raz. All samples were filtered
144 immediately after being collected using a 0.7 µm GF/F filter (Sigma-Aldrich) and kept on dry ice during transport
145 until they were frozen at -4°C for laboratory analysis for Raz concentrations. All analyses took place within a week
146 after the end of each round of injections. At the laboratory, each sample was buffered to a pH of 8.5 (1:10 buffer-to-
147 sample) following Knapp et al. (2018). The fluorescence signals were measured with a Cary Eclipse Fluorescence
148 Spectrophotometer (Agilent Technologies) using excitation/emission wavelengths of 602/632 nm for Raz and
149 571/584 nm for Rru and converted to concentrations based on an 8-point calibration curve (R^2=0.99).

150 We monitored specific conductivity (SC) and temperature using Campbell Scientific CS547A sensors
151 connected to Campbell Scientific CR 1000 dataloggers, which recorded and stored those measurements every 10
152 minutes. From the grab samples, we measured chloride using a Dionex ICS-1000 Ion Chromatograph with
153 AS23/AG23 analytical and guard columns. Cl data were augmented with background-corrected SC data to model
154 conservative transport.

155 We monitored changes in stream stage every 10 minutes at the end of the study reach using pressure
156 transducers (Campbell Scientific CS420) connected to a datalogger (Campbell Scientific CR 1000). We used
157 established stage-discharge relationships specific for the study site, as provided by the site managers. The discharge
158 values reported in Table 1 represent mean values observed during a given experiment.

159 **2.2 Conservative transport modelling and metrics**

160 We calibrated the conservative transport parameters of the transient storage model presented in Equations 1
161 and 2 using Cl⁻ and streamwater electrical conductivity data observed at Sites A and B. For this, we used the Matlab
162 (The Mathworks Inc., Natick, Massachusetts) script from Knapp et al. (2018), which features a joint calibration of
163 conservative and reactive solutes through a non-linear, least squares optimization routine.

164 $$\frac{\partial c}{\partial t} = -u\frac{\partial c}{\partial x} + D\frac{\partial^2 c}{\partial x^2} - \frac{A_s}{A}\frac{\partial c_{ts}}{\partial t} + q_{in}c - \lambda_{mc}c \tag{1}$$

165 $$\frac{\partial c_{ts}}{\partial t} = k(c - c_{ts}) - \lambda_{ts}c_{ts} \tag{2}$$

166

167 where c [ML^{-3}] and, c_{ts} [ML^{-3}] are the concentrations in the main channel and aggregate transient storage zone; x

168 [L] is the distance of the study reach; t [T] is time; u [LT^{-1}] and D [L^{2}T^{-1}] are parameters representing advective

169 flow velocity and dispersion coefficient, respectively; q_{in} [T^{-1}] is a volumetric flux parameter accounting for lateral

170 inputs; $k[T^{-1}]$ is the first-order mass transfer rate coefficient parameter between the main channel and the aggregate

171 transient storage zone; A_s/A [$-$] is the capacity ratio parameter representing the relative contribution of transient

172 storage-dominated to advection-dominated compartments in the stream, represented as areas along the reach; and

173 λ_{mc} and λ_{ts} [T^{-1}] are processing-rate coefficients in the main channel and transient storage zones (equaling zero for

174 a conservative tracer).

175   We completed the parameter estimation using the Differential Evolution Adaptive Metropolis (DREAM

176 [ZS]) algorithm (Vrugt et al. 2009). We jointly fit Cl$-$ and Raz data in a first step of 100,000 model generations. We

177 assessed model convergence using Gelman and Rubin $\hat{R}$ statistics (Gelman and Rubin 1992). The goodness of fit

178 between measured and simulated BTCs was quantified through the calculation of the residual sum of squares,

179 (nRSS) ($-$), normalized by the squared theoretical peak tracer concentrations of each tracer BTC of the respective

180 tracer at the given location. The medians of the best 1,000 model simulations were used to assess the agreement

181 between our final model fits and a subset of possible curve fits. The details on the model calibration procedure that

182 we use in this work were presented in the supporting information of Gootman et al. (2020). Examples of observed

183 and fitted breakthrough curves can be found in Figures S1-S3.

184   We estimated conservative transport timescales from the transport parameters to describe the transient

185 storage timescale, $\tau_{sz} = 1/k$ [T], and the mean travel time between sites A and B, τ [T], which was computed as:

186 $\tau = \frac{m_{1,cl}}{m_{0,cl}}$ (3)

187 $m_n = \sum_{i=1}^{r} \left(\frac{t_i+t_{i+1}}{2}\right)^n \left(\frac{C_i+C_{i+1}}{2}\right)(t_{i+1}-t_i)$ (4)

188 where $m_{0,cl}$ and $m_{1,cl}$ are the zeroth and first-centralized temporal moments of the Cl$^-$ BTCs from each sampling

189 site, i is a time index, r is the total number of samples available in a BTC.

2.3 Estimating the transformation of Raz as a proxy for microbial respiration:

191   We used the net transformation rate coefficients of Raz, λ_{Raz} [T^{-1}], as a proxy for microbial respiration.

192 λ_{Raz} incorporates transformation in the main channel and in transient storage zones, and was estimated following

193 the work by González-Pinzón and Haggerty (2013), who derived algebraic relationships with analytical solutions to

194 calculate processing rate coefficients from the transient storage model presented in Equations 1 and 2:

195 $\lambda_{Raz} = \frac{\ln\left(m_{0,Raz}^{inj}/m_{0,Raz}^{BTC}\right)}{\tau}\left(1 + \overbrace{\frac{\ln\left(m_{0,Raz}^{inj}/m_{0,Raz}^{BTC}\right)}{Pe}}^{dispersion\ term, \Phi}\right)$ (5)

196 where $m_{0,Raz}^{inj} = M_{Raz}/Q$ is the zeroth temporal moment of Raz at the injection site [M L^{-3} T^{-1}], M_{Raz} is the mass of

197 Raz added to the injectate, Q is the stream discharge [L^{3}T^{-1}]; $m_{0,Raz}^{BTC}$ is the dilution-corrected zeroth temporal

198 moment of Raz estimated with BTC data from a sampling site; and $Pe = L\,u/D$ is the Peclet number [-], which

199 describes the relative importance of advection and dispersion in the system. As noted by González-Pinzón and

200 Haggerty (2013), when $Pe \gg 10$, which is the case in advection-dominated systems such as open channel flow, the

201 dispersion term Φ is negligible and $\lambda_{Raz} \approx \ln(m_{0,Raz}^{inj}/m_{0,Raz}^{BTC})/\tau$.

202   Since we can only get one transformation rate coefficient from every observed BTC available from

203 Equation (5), or from the direct calibration of the transient storage model, we used the Tracer Addition for Spiraling

204 Curve Characterization (TASCC) framework (Covino et al. 2010b) to characterize uptake kinetics over the range of

205 experimental concentrations observed. In TASCC, the ratio of reactive to conservative solute concentrations for

206 every independent sample across the tracer BTCs is compared to the ratio of the concentrations of the injection

207 solution to determine uptake metrics. If the added solutes are non-reactive, they will transport conservatively, and

208 the ratio of the reactive to conservative solute concentrations will remain constant. Alternatively, if the added solutes

209 are limiting, co-limiting or reactive, they will not transport conservatively, and the ratio of the reactive to

210 conservative solute concentrations will change over time as a function of reactivity. TASCC-based transformation

211 rate coefficients for Raz were estimated using:

212 $\lambda_{Raz,sample} = \dfrac{\ln\left[\frac{C_{Raz}}{C_{cons.}}\right]_{inj} - \ln\left[\frac{C_{Raz}}{C_{cons.}}\right]_{BTC}}{x/u}$.   (6)

213   From each transformation rate coefficient λ_{Raz} and $\lambda_{Raz,sample}$, we also estimated an uptake (or mass

214 transfer) velocity of Raz, $V_{f_{Raz}} = \lambda_{Raz}h$ or $V_{f_{Raz,sample}} = \lambda_{Raz,sample}h$, where h is the mean depth of the stream.

215 Following Ensign and Doyle (2006), uptake velocities represent the vertical velocity of solute molecules through the

216 water column towards the benthos and are typically used in stream ecology to normalize processing-rate coefficients

217 by the influence from contrasting discharge magnitudes to facilitate the comparison of results from small streams

218 and large rivers. As demonstrated in Covino et al. (2010b), the range of $\lambda_{Raz,sample}$ and $V_{f_{Raz,sample}}$ values

219 encompass the λ_{Raz} and $V_{f_{Raz}}$ values obtained from processing rates derived from temporal moments analyses (e.g.,

220 Equation (5)).

221   Finally, reach-scale Damköhler numbers, Da [-], were calculated using the following equation:

222 $Da = \dfrac{transient\ storage\ timescale}{transformation\ timescale} = \tau_{sz}\lambda_{Raz}$.   (7)

223 **2.4 Statistical tests**

224   We calculated standard deviations (std) based on repeated measures of the distribution of the transport

225 parameters of Equations 1 and 2 to create upper and lower boundaries of the uncertainties in our measurements (i.e.,

226 mean ± std). Because our data were not normally distributed, we used the Mann-Whitney U nonparametric statistical

227 test to determine if there were statistically significant differences between nutrient treatments across rounds (e.g., N

228 vs. N in rounds 1 and 2), following a similar procedure in Ensign and Doyle (2006). For the Mann-Whitney U test,

229 we set our significance level (α, alpha) equal to 0.05.

230   We explored the Pearson correlation coefficient (r) matrix between the transport parameters of Equations 1

231 and 2, and associated metrics, to establish direct ($r > 0.1$), inverse ($r < -0.1$), and non-existent correlations ($-0.1 < r$

232 < 0.1) (Bowley 2008). We classified the strength of the correlations as uncorrelated ($0 < r < |0.1|$), weakly correlated

233 ($|0.1| < r < |0.5|$), moderately correlated ($|0.5| < r < |0.8|$), strongly correlated ($|0.8| < r < |1.0|$), and included p-values for

234 each correlation.

235   Lastly, we tested differences in mean values of the transport parameters of Equations 1 and 2, and

236 associated metrics, between nutrient treatments within each experimental round (e.g., N vs. N+C vs. N+P vs.

237 C+N+P in round 1) using the Student's *t*-test based on deviation from the group's mean value (Blair et al. 1980).

3 Results and Discussion

3.1 Conservative transport and metrics of physical controls

240   Between experimental rounds 1 and 2, stream depth (h) and discharge (Q) decreased, causing significant

241 differences in stream velocity (u), dispersion (D), mass-transfer rate coefficients (k), transient storage time scales

242 (τ_{TS}) and mean travel times (τ) (Figure 2). The only parameter that did not show significant differences was the

243 relative contribution of the main channel to storage zone areas, A_s/A.

244
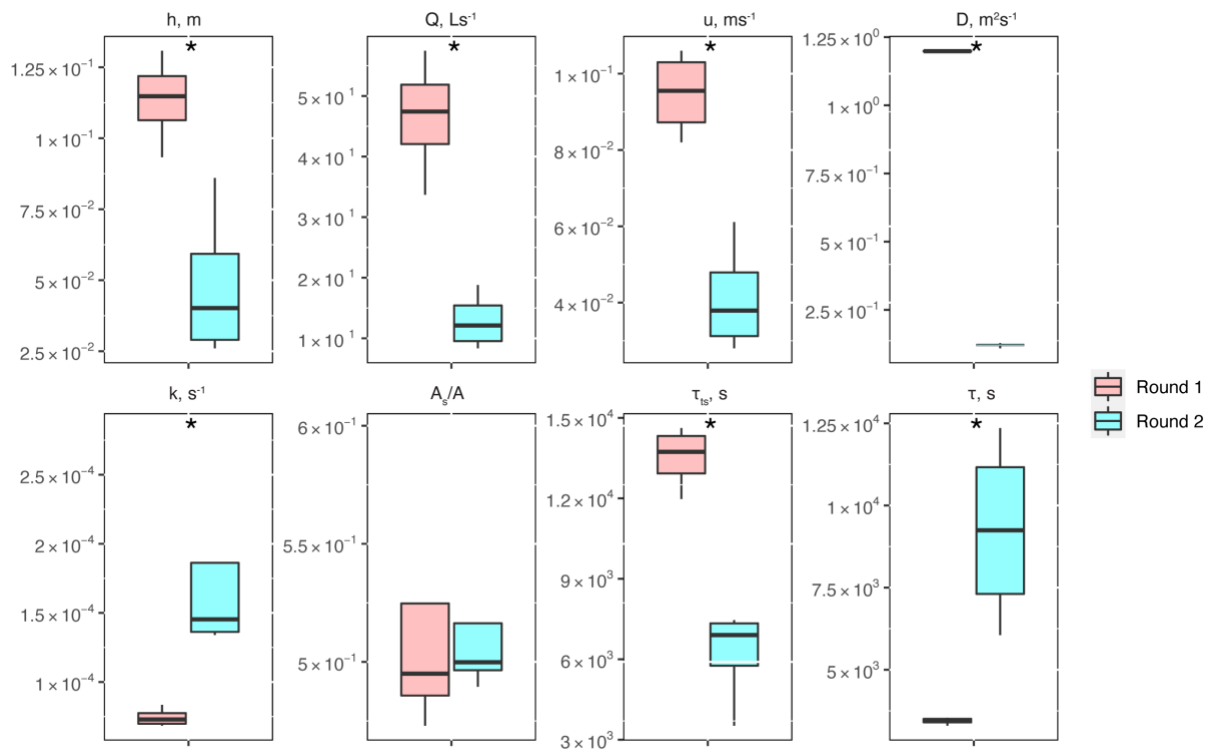
Figure 2: Conservative transport parameters and metrics of physical controls estimated for the two experimental rounds: stream depth (h), stream velocity (u), dispersion (D), mass transfer rate coefficients (k), the ratio of transient storage-dominated to advection-dominated compartments (A_s/A), transient storage time scales (τ_{TS}) and mean travel times (τ). Asterisks represent statistical differences in magnitudes for rounds 1 and 2 with p<0.05 (*) based on the Mann-Whitney U nonparametric statistical test.

252   The correlation matrix between parameters and metrics (Figure 3) shows that Q (and interrelated quantities

253 h and u), D, and τ_{ts} were all directly correlated (from moderately to strongly). Mean travel times between sites, τ,

254   were directly and weakly correlated with k and the ratio A_s/A, and inversely correlated (from weakly to strongly)

255   with the rest of the conservative transport parameters and metrics. Finally, the ratio A_s/A was generally uncorrelated

256   or weakly correlated with other quantities. Even though the correlations of some interdependent quantities are

257   known to be spurious, e.g., Q vs. u and λ_{Raz} vs. $V_{f_{Raz}}$ (González-Pinzón et al. 2015), we included all relevant

258   measured and modeled quantities in Figure 3 to allow readers to explore different data pairs. For clarity, we

259   differentiate with brackets all known spurious correlations. Note that we did not flag the correlation between A_s/A

260   and Q (and their interrelated quantities h and u) as spurious because the ratio of areas is an indicator of the relative

261   volume-based contribution from advection-dominated to transient storage-dominated compartments, instead of

262   actual estimates of cross-sectional areas (Kelleher et al. 2013; González-Pinzón et al. 2013; Knapp and Kelleher

263   2020).

264
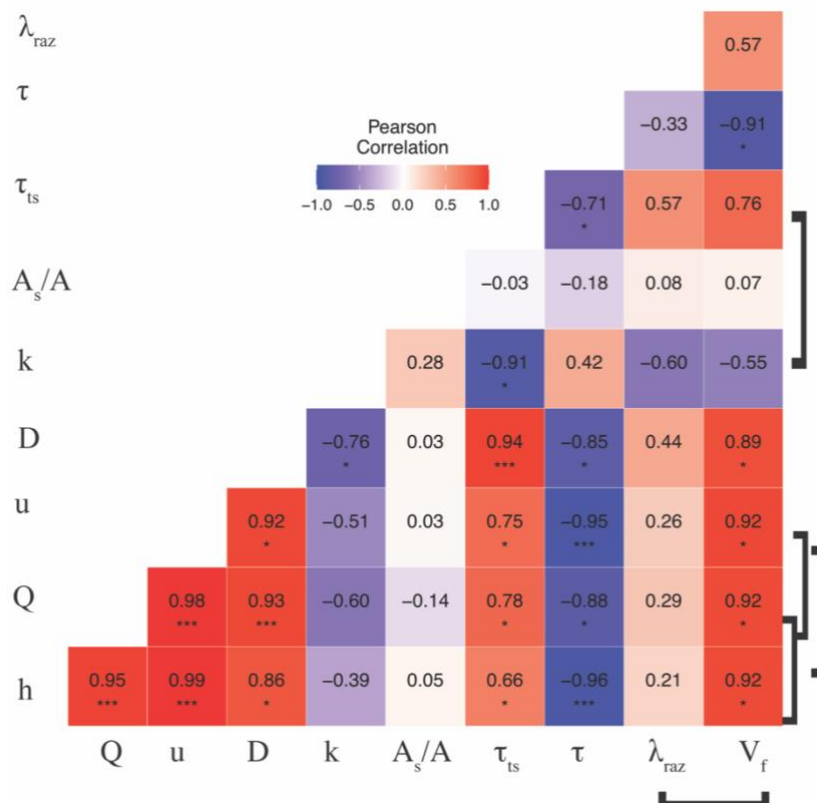
265
266   **Figure 3: Pearson correlation coefficient (r) heatmap for the mean values of the transport parameters and metrics for**
267   **each stoichiometric treatment during rounds 1 and 2. Brackets link known spurious correlations. Asterisks represent**
268   **significant differences in magnitudes between parameters with p<0.05 (*), and p<0.001(***) based on the Pearson**
269   **Correlation.**

270
271   One of the metrics of interest in stream reactive-transport modeling is the transient storage timescale ($\tau_{ts} =$

272    $1/k$), which quantifies the exposure that solutes have to biological communities in metabolically active transient

273   storage zones. In our study site, τ_{ts} decreased one order of magnitude from round 1 to round 2, and were comparable

274   to the range of values observed in other studies involving forested mountain streams (Valett et al. 1996; Hall et al.

275   2002). Due to the geomorphology of the stream, which is characterized by pool and riffle sequences, but steep

276   longitudinal and valley slopes and shallow bedrock, transient storage was expected to occur mainly in the main

277   channel (Fields and Dethier 2019; Barnhart et al. 2021; Emanuelson et al. 2022). As flow receded from round 1 to

278   round 2, we observed the disconnection of in-stream pools contributing to transient storage, which explains the

279   direct correlation between discharge and transient storage timescales. Another indication of the dominant

280   contribution of in-stream pools to total transient storage is the lack of change of A_s/A with discharge. Since A is

281   expected to vary proportional with discharge (i.e., $Q = A \cdot u$), a constant A_s/A suggests that the contribution of

282   transient storage-dominated (i.e., A_s) compartments (i.e., A) also varied proportionally with discharge.

3.2 Raz transformation (a proxy for respiration) as a function of physical controls

284   Our results indicate that the mean values of the transformation rate coefficient of Raz (λ_{Raz}) were directly

285   and moderately correlated with the transient storage timescale (τ_{ts}), as other studies on reactive transport have

286   shown (Valett et al. 1996; Hall et al. 2002; Gomez et al. 2012; Zarnetske et al. 2012; Kiel and Bayani Cardenas

287   2014; Gootman et al. 2020). Mean λ_{Raz} values were directly and weakly correlated with discharge (Q) (also depths

288   h and velocities u) and dispersion (D), and directly and moderately correlated with τ_{ts}. Mean λ_{Raz} values were

289   inversely and weakly correlated with mean travel times (τ), and inversely and moderately correlated with mass-

290   transfer rate coefficients (k) (Figure 3). Raz uptake velocities ($V_{f_{Raz}}$) showed spurious, direct and strong

291   correlations with discharge (Q) (also h and u), strong correlations with dispersion (D) and transient storage

292   timescales (τ_{ts}), and strong indirect correlations with mean travel times (τ) and k (moderate). Finally, both λ_{Raz} and

293    $V_{f_{Raz}}$ were uncorrelated with A_s/A. Unlike studies where an increased transient storage timescale (τ_{ts}) is mainly

294   associated with slower hyporheic flows due to lower discharges (Q) (Zarnetske et al. 2007; Schmid et al. 2010), τ_{ts}

295   in our study site increased with Q because the geomorphology of the channel and the valley favored in-stream

296   transient storage in lateral pools (Jackson et al. 2012, 2013, 2015). Similar declines in transient storage with falling

297   discharge have been observed in other streams with comparable geomorphic characteristics (Covino et al. 2010a;

298   Emanuelson et al. 2022), however, the absence of concurrent declines in respiration suggest biological control by

299   some other mechanism.

3.3 Raz transformation (a proxy for respiration) as a function of physical and stoichiometric controls

301   Our results suggest no significant changes in respiration despite significant differences in discharge (Q),

302   temperature, and nutrient treatments. Between experimental rounds, the mean values of Q (and h and u by

303   extension) and temperature (except for N+C) were statistically different for each treatment comparison (Figure 4A).

304   For $\lambda_{Raz,sample}$, we only found statistical differences between rounds for the C+N+P treatments (Figure 4C). Due to

305   the large influence of Q on the uptake velocity of Raz ($V_{f_{Raz,sample}}$) through stream depth (h), the statistical

306   differences between rounds seen for Q were also seen for $V_{f_{Raz,sample}}$ (Figure 4D).

307
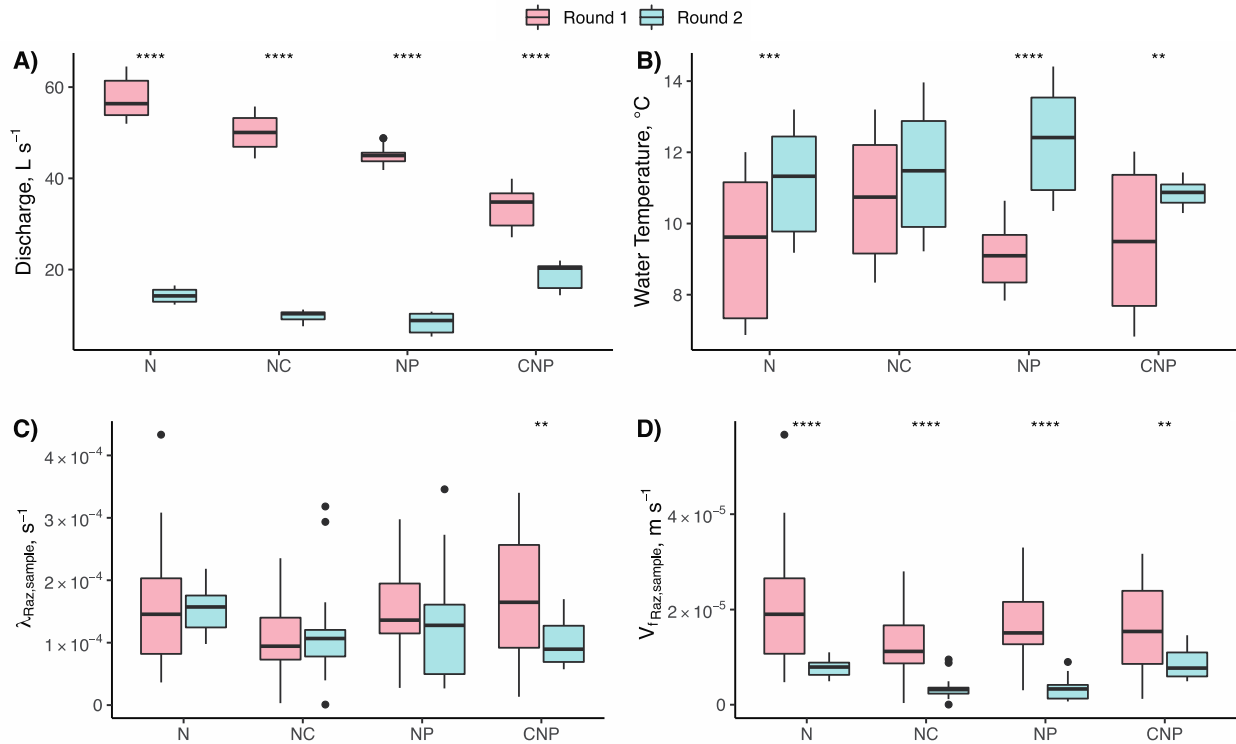
Figure 4: Comparison of A) stream discharge values recorded at the gaging station, B) stream water temperatures, C) transformation rate coefficients of resazurin ($\lambda_{Raz,sample}$) resulting from Equation 6, and associated D) uptake velocities of resazurin ($V_{f_{Raz,sample}} = \lambda_{Raz,sample} \, h$) estimated for each experimental nutrient treatment addition during rounds 1 and 2. Due to the large influence of Q on the uptake velocity of Raz ($V_{f_{Raz,sample}}$) through stream depth (h), most of the statistical differences between rounds seen for Q were also seen for $V_{f_{Raz,sample}}$. Asterisks represent significant differences in magnitudes between rounds with p<0.01(**), and p~0 (****) based on the Mann-Whitney U nonparametric statistical test.

When looking at the data collected from each round, we found that mean Q values were statistically different across nutrient treatments (Figures 5A and 5D). For mean $\lambda_{Raz,sample}$ values, the only treatments with statistical differences were the N+C and C+N+P from round 1 (Figures 5B and 5E). Finally, $V_{f_{Raz,sample}}$ mean values were only statistically different for the N vs N+C treatments for round 1, and for all but the N+C vs N+P and N vs C+N+P treatments for round 2 (Figures 5C and 5F).
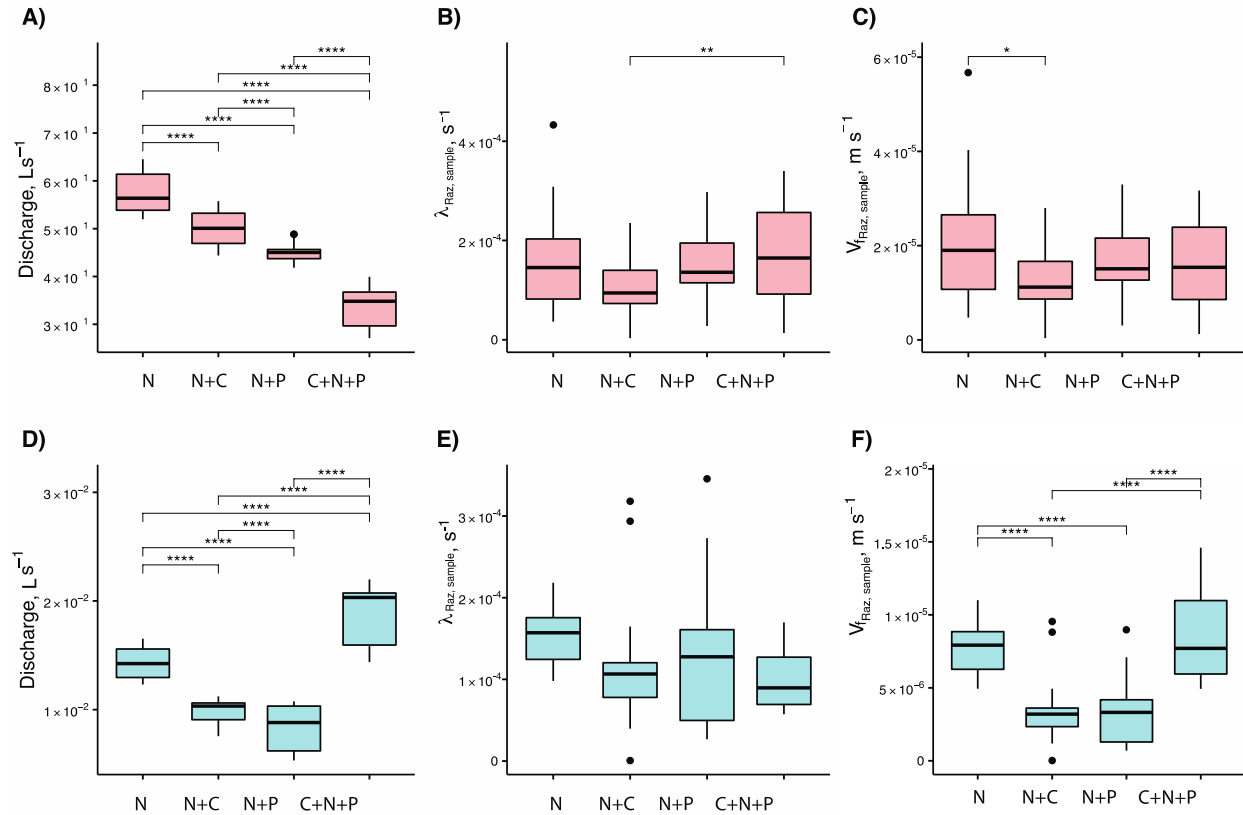
323
324 **Figure 5: Comparison of stream discharges (A and D), transformation rate coefficients of resazurin ($\lambda_{Raz,sample}$) resulting**
325 **from Equation 6 (B and E), and associated uptake velocities of resazurin ($V_{f_{Raz,sample}}$) (C and F) across treatments for**
326 **round 1(top row) and 2 (bottom row). Due to the large influence of Q on the uptake velocity of Raz ($V_{f_{Raz,sample}}$) through**
327 **stream depth (h), most of the statistical differences between rounds seen for Q were also seen for $V_{f_{Raz,sample}}$. Asterisks**
328 **represent significant differences in magnitudes for treatments N, N+C, N+P, and C+N+P with p<0.05 (*), p<0.01(**), and**
329 **p~0 (****) based on the Mann-Whitney U nonparametric statistical test.**
330
331   For each of the eight nutrient injections, we related the mean transient storage timescales at the reach scale,
332 τ_{ts}, which indicate exposure times between solutes and microbial communities, and the mean transformation
333 timescales of Raz at the reach scale, $1/\lambda_{Raz}$, which indicate respiration (Figure 6). This Damköhler-based analysis
334 allows us to visualize the interplay between physical, biological, and stoichiometric controls in the stream. We found
335 that the range of variation of the mean transient storage timescales was three times greater than that of the mean
336 transformation timescales. In round 1, all the stoichiometric treatments resulted in transport-limited conditions due
337 to the high values of τ_{ts}, i.e., the average particle of Raz that entered a metabolically active compartment underwent
338 transformation and more Raz could have been transformed if it had been available. Thus, in round 1, respiration was
339 high relative to the supply of solutes to the metabolically active transient storage zones. In round 2, all
340 stoichiometric treatments, except N, resulted in reaction-limited conditions, i.e., the average particle of Raz entering
341 a metabolically active compartment left it without undergoing transformation. Thus, in round 2, respiration was slow
342 relative to the exposure of solutes to microbial communities.
343
344
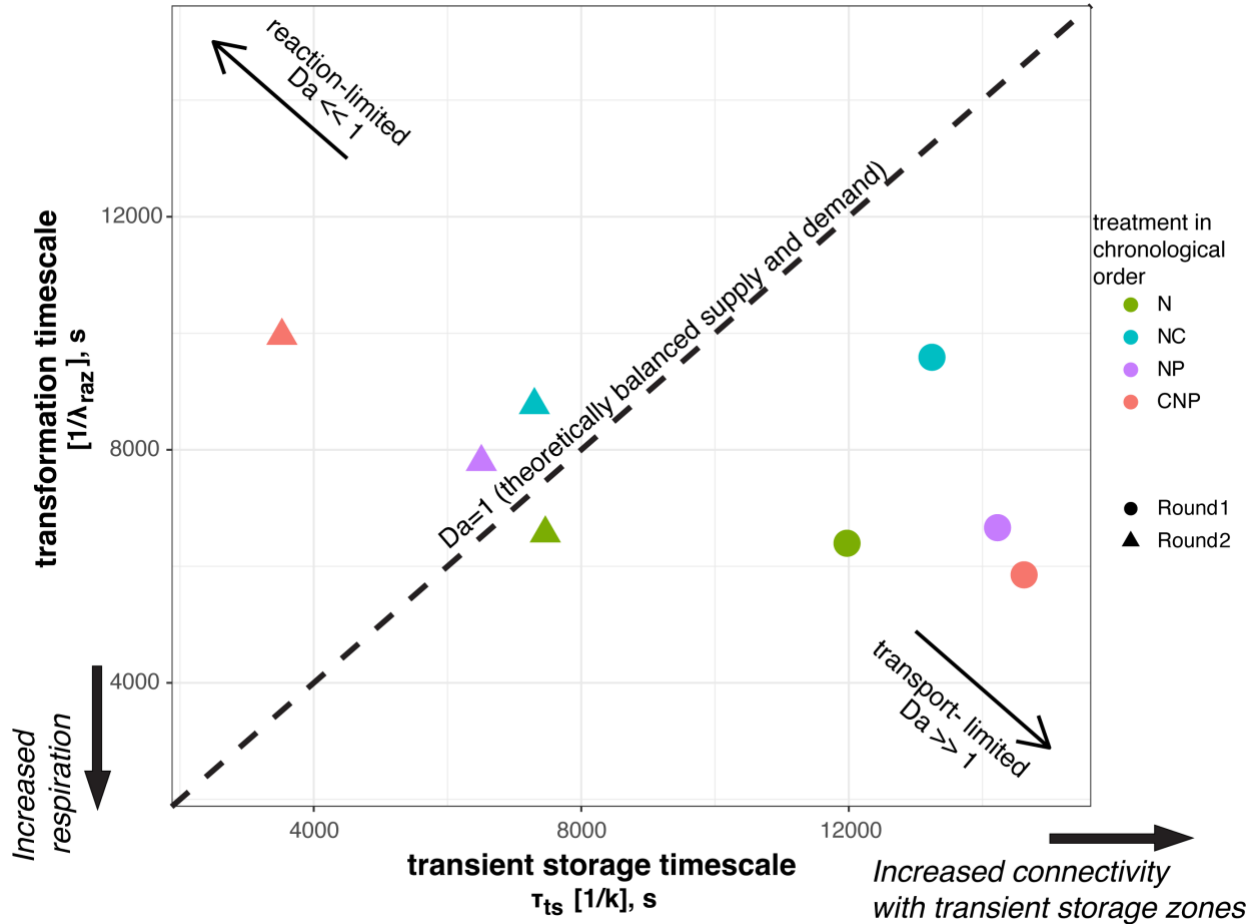
Figure 6: Mean reaction and transient storage timescales for each nutrient treatment. The Damköhler, $Da =$ transient storage timescale/ transformation timescale, indicates reaction-limited and transport-limited conditions.

3.4 How is microbial respiration controlled by hydrologic exchange vs. stoichiometric conditions (i.e., supply of C, N, and P)?

We characterized reach-scale microbial respiration with the transformation timescale of Raz, $1/\lambda_{Raz}$; the extent of hydrologic exchanges along the reach with the transient storage timescale, τ_{TS}, and the relative size of the main channel and transient storage areas, A_s/A; and stoichiometric conditions with our controlled nutrient additions (i.e., N, N+C, N+P, and C+N+P treatments). The most salient findings indicate that a) discharge (Q) changed significantly between rounds (Figure 4a) and across stoichiometric treatments (Figure 5a, 5d), and was directly and moderately correlated with τ_{TS} and uncorrelated with A_s/A (Figure 3), suggesting that most transient storage occurred in lateral pools in the channel, which increased in quantity and extent proportionally with Q, and b) the respiration activity indicated by λ_{Raz} remained similar between rounds with significantly different Q (Figure 4b), and across controlled stoichiometric treatments also featuring different Q (Figure 5b, 5e). Thus, we observed that respiration remained largely unchanged or constant with varying physical and stoichiometric conditions.

Several hypotheses may explain the invariant reach-scale respiration observed between experimental rounds and treatments. First, tradeoffs in metabolic rates may have occurred as the stream shifted from high to low

363 flows. At high flows during late June and early July, lateral pools in the main channel were inundated, and transient

364 storage timescales likely associated with these pools were high. Under these conditions, the observed respiration was

365 probably supported by low levels of processing in the hyporheic zone due to the prevalence of bedrock substrate and

366 relatively low respiration from benthic biomass due to scour from high flows (Francoeur and Biggs 2006; Katz et al.

367 2018). However, the combination of longer transient storage timescales and an expanded total surface area resulted

368 in moderate total respiration. In contrast, during the low flows seen in the second round of injections, surface area,

369 and transient storage timescales were decreased due to the contraction of the channel. Under these conditions,

370 biomass increased likely due to decreased scour and increased stability (Francoeur and Biggs 2006; Katz et al. 2018;

371 Cargill et al. 2021), increased water temperatures (Perkins et al. 2012), and increased processing of autochthonous

372 carbon (Wagner et al. 2017) (Figure S4). This may have supported elevated areal metabolic rates in benthic biofilms

373 (Battin et al. 2016), maintaining relatively constant respiration levels with respect to the first round of injections.

374 An alternative hypothesis to explain the consistency of the observed respiration values is that some other

375 factor constraints respiration values within a narrow range. For example, the limitation of a key nutrient or metabolic

376 resource may constrain respiration. While we designed the experiments to relieve stoichiometric constraints, it is

377 possible that the quantities of C, N, and P in the injectate we were logistically able to introduce to the stream were

378 insufficient to overcome demand. Also, the form of the resources may not have been readily available to

379 communities adapted to these locals, as stream microbial communities most efficiently process the forms and

380 diversity of dissolved organic matter found in their native habitats, and they express extracellular enzymes in ratios

381 appropriate to acquire limiting nutrients (Hill et al. 2012; Lane et al. 2012; Wilhelm et al. 2015; Logue et al. 2016).

382 In previous studies, transient storage and nutrient uptake have presented contradictory relationships, which

383 we summarize below.

384 *Inconclusive relationships:* Martí et al. (1997) did not find correlations between NH_3 uptake length and

385 A_s/A in a desert stream using data from eight tracer injections. Webster et al. (2003) did not find statistically

386 significant relationships between NH_4 uptake and A_s/A using the 11-stream LINX-I dataset that included arctic to

387 tropical streams. From thirty seven injections conducted in thirteen streams at Hubbard Brook Experimental Forest

388 (HBEF), Hall et al. (2002) found weak correlations (R^2=0.14-0.35) between transient storage parameters and NH_4

389 demand. Using data from seven streams in New Zealand, Niyogi et al. (2004) did not find significant correlations

390 between soluble reactive phosphorous (P-SRP), NO_3 uptake velocities, and A_s/A. Bukaveckas (2007) reported an

391 indefinite relationship between transient storage and NO_3 and P-SRP retention efficiencies from tracer injections in a

392 reference (N=13 injections), a channelized (N=14 injections), and a restored (N=17 injections) stream reach in the

393 midwestern US. Lastly, the LINX-II dataset from ^{15}N-NO_3 injections in 72 streams located in eight regions of the

394 US showed no relationship between NO_3 uptake and the fraction of median travel time due to transient storage

395 (F_{med}^{200}) (Hall et al. 2009).

396 *Weak to moderate relationships:* Thomas et al. (2003) showed that transient storage accounted for 44% to

397 49% of NO_3 retention measured by ^{15}N in a small headwater stream in North Carolina. Mulholland et al. (1997)

398 found larger PO_4 uptake rates in a stream with higher transient storage, when they compared two forested streams.

399 Ensign and Doyle (2005) found an increase in A_s/A and the uptake velocities for NH_4 and PO_4 after the addition of

400 flow baffles to two streams. Lautz and Siegel (2007) found a modest correlation (R^2=0.44) between NO_3 retention
401 efficiency and transient storage in the Red Canyon Creek watershed, WY.

402   *Strong relationships:* Valett et al. (1996) found a strong correlation (R^2=0.77) between transient storage
403 and NO_3 retention in three first-order streams in New Mexico. From nine tracer injections in two urban streams in
404 the eastern US, Ryan et al. (2007) found strong relationships between P-SRP retention and transient storage metrics
405 ($k, A_s/A$; R^2>0.84) when the variables were measured in different seasons. Sheibley et al. (2014) observed that the
406 retention of NO_3 in seven agricultural streams in the US was positively correlated with A_s/A and the average water
407 flux through the storage zone per unit length of stream ($q_s = kA$), and negatively correlated with the transient
408 storage timescale (τ_{ts}). However, they found no significant correlation between NH_4^+ and SRP retention and
409 transient storage metrics.

410   The studies referenced above were performed in streams with contrasting physical, chemical, and
411 biological conditions. Together, they offer a broader perspective on the inconsistent relationship between transient
412 storage metrics and metabolic processing. Those studies do not feature co-injections of C, N, and P macronutrients
413 (e.g., N+C, N+P, N+C+P), even while some tracked ambient processing rates of more than one nutrient. Therefore,
414 they generally represent solute-specific analyses, where the uptake of one nutrient at a time was analyzed and, thus,
415 did not account for stoichiometric controls on nutrient uptake (however, see Tromboni et al. (2018) for an example
416 of recent trend changes in this research area). By combining both transport and stoichiometric analyses, our study
417 offers evidence that stoichiometric controls have an ambiguous relationship to reach-scale metabolic activities, and
418 that further investigations should be conducted using greater quantities and types of resources.

419 **4 Conclusions**

420   We conducted two rounds of four stoichiometric treatments (i.e., N, C+N, N+P, and C+N+P) in a
421 headwater stream in Colorado to quantify reach-scale changes to stream respiration during flow recession and
422 answer the question: *How is respiration controlled by hydrologic exchange vs. stoichiometric conditions (i.e., supply
423 of C, N, and P)?* We found that discharge changed significantly between rounds and across stoichiometric
424 treatments, and that it was directly and moderately correlated with transient storage timescales but uncorrelated with
425 the ratio of contributions from advection-dominated to transient storage-dominated compartments (i.e., A_S/A). This
426 suggests that most transient storage occurred in lateral pools within the main channel, which increased in quantity
427 and extent proportionally with discharge. We also found that respiration remained similar despite significant
428 changes in discharge and stoichiometric treatments. Our results contradict the notion that hydrologic transport alone
429 is a dominant control on biogeochemical processing, and suggest that complex interactions between hydrology,
430 resource supply, and biological community function are responsible for driving in-stream respiration.

431 **Author contribution:** RGP, TC, KS, and MG secured the funding for this research. All co-authors designed carried
432 out the experiments. JD and RGP processed Raz samples, performed solute transport simulations, statistical analyses,

433 and prepared the manuscript with input from all co-authors. DVH supported the contextualization of hydrological and

434 ecological interactions. All co-authors approved the final version of the manuscript.

435 **Competing interests:** The authors declare no competing interests.

436 **Acknowledgments**

437 The National Science Foundation provided funding support through grants NSF EAR-1642399, NSF EAR-
438 1642368, NSF EAR-1642402, NSF EAR-1642403, and NSF 1914490. We thank Karin Emanuelson, Jackie
439 Randell, Erin Jenkins, Tristan Weiss, and Melissa Pinzon for their field and laboratory assistance.

440 **Data availability:** The data used in his article can be found in the CUAHSI HydroShare repository. Gonzalez-Pinzon,
441 R. (2022). Resazurin tracer data from experiments in Colorado (2018) and Iowa (2019),
442 HydroShare, http://www.hydroshare.org/resource/50ae3c59bebe4cb383e31408a0c10012

443
444
445
446

References

447 **References**

448 Barnhart, T. B., J. Vukomanovic, P. Bourgeron, and N. P. Molotch. 2021. Future land cover and
449   climate may drive decreases in snow wind-scour and transpiration, increasing streamflow
450   at a Colorado, USA headwater catchment. Hydrol. Process. **35**: e14416.
451   doi:10.1002/hyp.14416
452 Battin, T. J., K. Besemer, M. M. Bengtsson, A. M. Romani, and A. I. Packmann. 2016. The
453   ecology and biogeochemistry of stream biofilms. Nat. Rev. Microbiol. **14**: 251–263.
454   doi:10.1038/nrmicro.2016.15
455 Battin, T. J., L. A. Kaplan, J. D. Newbold, and C. M. E. Hansen. 2003. Contributions of
456   microbial biofilms to ecosystem processes in stream mesocosms. Nature **426**: 439–442.
457   doi:10.1038/nature02152
458 Blair, R. C., J. J. Higgins, S. Journal, and N. Winter. 1980. A Comparison of the Power of
459   Wilcoxon ' s Rank-Sum Statistic to That of Student ' s t Statistic under Various
460   Nonnormal Distributions Published by : American Educational Research Association and
461   American Statistical Association Stable URL : https://www.jstor.org/stable/1164905
462   REFERENCES Linked references are available on JSTOR for this article : reference #
463   references _ tab _ contents You may need to log in to JSTOR to access the linked
464   references . **5**: 309–335.
465 Blume, E., M. Bischoff, J. M. Reichert, T. Moorman, A. Konopka, and R. F. Turco. 2002.
466   Surface and subsurface microbial biomass, community structure and metabolic activity as
467   a function of soil depth and season. Appl. Soil Ecol. **20**: 171–181. doi:10.1016/S0929-
468   1393(02)00025-2
469 Bowley, A. L. 2008. The Standard Deviation of the Correlation Coefficient Author (s): A . L .
470   Bowley Source : Journal of the American Statistical Association , Vol . 23 , No . 161 (
471   Mar ., 1928), pp . 31- Published by : American Statistical Association Stable URL :
472   http:/. J. Am. Stat. Assoc. **23**: 31–34.
473 Bukaveckas, P. A. 2007. Effects of Channel Restoration on Water Velocity, Transient Storage,
474   and Nutrient Uptake in a Channelized Stream. Environ. Sci. Technol. **41**: 1570–1576.
475   doi:10.1021/es061618x
476 Cardenas, M. B., J. L. Wilson, and V. A. Zlotnik. 2004. Impact of heterogeneity, bed forms, and
477   stream curvature on subchannel hyporheic exchange. Water Resour. Res. **40**: 1–14.
478   doi:10.1029/2004WR003008
479 Cargill, S. K., C. Segura, S. R. Villamizar, and D. R. Warren. 2021. The influence of lithology
480   on stream metabolism in headwater systems. Ecohydrology **14**. doi:10.1002/eco.2284
481 Covino, T. P., B. McGlynn, and M. Baker. 2010a. Separating physical and biological nutrient
482   retention and quantifying uptake kinetics from ambient to saturation in successive
483   mountain stream reaches. J. Geophys. Res. Biogeosciences **115**: 1–17.
484   doi:10.1029/2009JG001263
485 Covino, T. P., and B. L. McGlynn. 2007. Stream gains and losses across a mountain-to-valley
486   transition: Impacts on watershed hydrology and stream water chemistry. Water Resour.
487   Res. **43**: 1–14. doi:10.1029/2006WR005544
488 Covino, T. P., B. L. Mcglynn, and R. A. Mcnamara. 2010b. Tracer Additions for Spiraling Curve
489   Characterization (TASCC): Quantifying stream nutrient uptake kinetics from ambient to
490   saturation. Limnol. Oceanogr. Methods 484–498. doi:10.4319/lom.2010.8.484
491 Covino, T. P., B. McGlynn, and J. Mallard. 2011. Stream-groundwater exchange and hydrologic
492   turnover at the network scale. Water Resour. Res. **47**: 1–11. doi:10.1029/2011WR010942

Dallan, E., P. Regier, A. Marion, and R. González-Pinzón. 2020. Does the Mass Balance of the Reactive Tracers Resazurin and Resorufin Close at the Microbial Scale? J. Geophys. Res. Biogeosciences **125**: 1–10. doi:10.1029/2019JG005435

Emanuelson, K., T. P. Covino, A. S. Ward, J. Dorley, and M. N. Gooseff. 2022. Conservative solute transport processes and associated transient storage mechanisms: Comparing streams with contrasting channel morphologies, land use and land cover. Hydrol. Process. **36**.

Ensign, S. H., and M. W. Doyle. 2005. In-channel transient storage and associated nutrient retention: Evidence from experimental manipulations. Limnol. Oceanogr. **50**: 1740–1751. doi:10.4319/lo.2005.50.6.1740

Ensign, S. H., and M. W. Doyle. 2006. Nutrient spiraling in streams and river networks. J. Geophys. Res. Biogeosciences **111**. doi:10.1029/2005jg000114

Fields, J. F., and D. P. Dethier. 2019. From on high: Geochemistry of alpine springs, Niwot Ridge, Colorado Front Range, USA. Hydrol. Process. **33**: 1756–1774. doi:10.1002/hyp.13436

Francoeur, S. N., and B. J. F. Biggs. 2006. Short-term Effects of Elevated Velocity and Sediment Abrasion on Benthic Algal Communities. Hydrobiologia **561**: 59–69. doi:10.1007/s10750-005-1604-4

Gelman, A., and D. B. Rubin. 1992. Inference from Iterative Simulation Using Multiple Sequences. Stat. Sci. **7**. doi:10.1214/ss/1177011136

Gomez, J. D., J. L. Wilson, and M. B. Cardenas. 2012. Residence time distributions in sinuosity-driven hyporheic zones and their biogeochemical effects. Water Resour. Res. **48**: 1–17. doi:10.1029/2012WR012180

González-Pinzón, R., J. Dorley, J. Singley, K. Singha, M. Gooseff, and T. Covino. 2022. TIPT: The Tracer Injection Planning Tool. Environ. Model. Softw. **156**: 105504. doi:10.1016/j.envsoft.2022.105504

González-Pinzón, R., and R. Haggerty. 2013. An efficient method to estimate processing rates in streams. Water Resour. Res. **49**: 6096–6099. doi:10.1002/wrcr.20446

González-Pinzón, R., R. Haggerty, and A. Argerich. 2014. Quantifying spatial differences in metabolism in headwater streams. Freshw. Sci. **33**: 798–811. doi:10.1086/677555

González-Pinzón, R., R. Haggerty, and M. Dentz. 2013. Scaling and predicting solute transport processes in streams. Water Resour. Res. **49**: 4071–4088. doi:10.1002/wrcr.20280

González-Pinzón, R., R. Haggerty, and D. D. Myrold. 2012. Measuring aerobic respiration in stream ecosystems using the resazurin-resorufin system. J. Geophys. Res. Biogeosciences **117**: 1–10. doi:10.1029/2012JG001965

González-Pinzón, R., J. Mortensen, and D. Van Horn. 2015. Comment on "Solute-specific scaling of inorganic nitrogen and phosphorus uptake in streams" by Hall et al. (2013). Biogeosciences **12**: 5365–5369. doi:10.5194/bg-12-5365-2015

González-Pinzón, R., M. Peipoch, R. Haggerty, E. Martí, and J. H. Fleckenstein. 2016. Nighttime and daytime respiration in a headwater stream. Ecohydrology **9**: 93–100. doi:10.1002/eco.1615

Gooseff, M. N., K. E. Bencala, D. T. Scott, R. L. Runkel, and D. M. McKnight. 2005. Sensitivity analysis of conservative and reactive stream transient storage models applied to field data from multiple-reach experiments. Adv. Water Resour. **28**: 479–492. doi:10.1016/j.advwatres.2004.11.012

Gooseff, M. N., D. M. McKnight, R. L. Runkel, and J. H. Duff. 2004. Denitrification and hydrologic transient storage in a glacial meltwater stream, McMurdo Dry Valleys, Antarctica. Limnol. Oceanogr. **49**: 1884–1895. doi:10.4319/lo.2004.49.5.1884

Gootman, K. S., R. G. Pinzón, J. L. A. Knapp, V. Garayburu-Caruso, and J. Cable. 2020. Spatiotemporal Variability in Transport and Reactive Processes Across a First - to Fifth - Order Fluvial Network Water Resources Research. 1–18. doi:10.1029/2019WR026303

Hall, R. J. O., E. S. Bernhardt, and G. E. Likens. 2002. Relating nutrient uptake with transient storage in forested mountain streams. Limnol. Oceanogr. **47**: 255–265. doi:10.4319/lo.2002.47.1.0255

Hall, R. O., J. L. Tank, D. J. Sobota, and others. 2009. Nitrate removal in stream ecosystems measured by 15N addition experiments: Total uptake. Limnol. Oceanogr. **54**: 653–665. doi:10.4319/lo.2009.54.3.0653

Harvey, J. W., J. K. Böhlke, M. A. Voytek, D. Scott, and C. R. Tobias. 2013. Hyporheic zone denitrification: Controls on effective reaction depth and contribution to whole-stream mass balance. Water Resour. Res. **49**: 6298–6316. doi:10.1002/wrcr.20492

Harvey, J. W., J. E. Saiers, and J. T. Newlin. 2005. Solute transport and storage mechanisms in wetlands of the Everglades, south Florida. Water Resour. Res. **41**. doi:10.1029/2004WR003507

Hill, B. H., C. M. Elonen, L. R. Seifert, A. A. May, and E. Tarquinio. 2012. Microbial enzyme stoichiometry and nutrient limitation in US streams and rivers. Ecol. Indic. **18**: 540–551. doi:10.1016/j.ecolind.2012.01.007

Jackson, T. R., S. V. Apte, R. Haggerty, and R. Budwig. 2015. Flow structure and mean residence times of lateral cavities in open channel flows: influence of bed roughness and shape. Environ. Fluid Mech. **15**: 1069–1100. doi:10.1007/s10652-015-9407-2

Jackson, T. R., R. Haggerty, S. V. Apte, A. Coleman, and K. J. Drost. 2012. Defining and measuring the mean residence time of lateral surface transient storage zones in small streams. Water Resour. Res. **48**. doi:10.1029/2012WR012096

Jackson, T. R., R. Haggerty, S. V. Apte, and B. L. O'Connor. 2013. A mean residence time relationship for lateral cavities in gravel-bed rivers and streams: Incorporating streambed roughness and cavity shape. Water Resour. Res. **49**: 3642–3650. doi:10.1002/wrcr.20272

Kasahara, T., and S. M. Wondzell. 2003. Geomorphic controls on hyporheic exchange flow in mountain streams. Water Resour. Res. **39**: SBH 3-1-SBH 3-14. doi:10.1029/2002wr001386

Katz, S. B., C. Segura, and D. R. Warren. 2018. The influence of channel bed disturbance on benthic Chlorophyll a: A high resolution perspective. Geomorphology **305**: 141–153. doi:10.1016/j.geomorph.2017.11.010

Kelleher, C., T. Wagener, B. McGlynn, A. S. Ward, M. N. Gooseff, and R. A. Payn. 2013. Identifiability of transient storage model parameters along a mountain stream. Water Resour. Res. **49**: 5290–5306. doi:10.1002/wrcr.20413

Kiel, B. A., and M. Bayani Cardenas. 2014. Lateral hyporheic exchange throughout the Mississippi River network. Nat. Geosci. **7**: 413–417. doi:10.1038/ngeo2157

Knapp, J. L. A., R. González-Pinzón, J. D. Drummond, L. G. Larsen, O. A. Cirpka, and J. W. Harvey. 2017. Tracer-based characterization of hyporheic exchange and benthic biolayers in streams. Water Resour. Res. **53**: 1575–1594. doi:10.1002/2016WR019393

582 Knapp, J. L. A., R. González-Pinzón, and R. Haggerty. 2018. The Resazurin-Resorufin System:
583   Insights From a Decade of "Smart" Tracer Development for Hydrologic Applications.
584   Water Resour. Res. **54**: 6877–6889. doi:10.1029/2018WR023103

585 Knapp, J. L. A., and C. Kelleher. 2020. A Perspective on the Future of Transient Storage
586   Modeling: Let's Stop Chasing Our Tails. Water Resour. Res. **56**: e2019WR026257.
587   doi:10.1029/2019WR026257

588 Krause, S., J. Lewandowski, N. B. Grimm, and others. 2017. Ecohydrological interfaces as hot
589   spots of ecosystem processes: ECOHYDROLOGICAL INTERFACES AS HOT SPOTS.
590   Water Resour. Res. **53**: 6359–6376. doi:10.1002/2016WR019516

591 Lane, C. S., D. R. Lyon, and S. E. Ziegler. 2012. Cycling of two carbon substrates of contrasting
592   lability by heterotrophic biofilms across a nutrient gradient of headwater streams. Aquat.
593   Sci. **75**: 235–250. doi:10.1007/s00027-012-0269-0

594 Lautz, L. K., and D. I. Siegel. 2007. The effect of transient storage on nitrate uptake lengths in
595   streams: an inter-site comparison. Hydrol. Process. **21**: 3533–3548. doi:10.1002/hyp.6569

596 Li, L., P. L. Sullivan, P. Benettin, and others. 2021. Toward catchment hydro-biogeochemical
597   theories. Wiley Interdiscip. Rev. Water **8**: 1–31. doi:10.1002/wat2.1495

598 Li, Z., Z. Zeng, D. Tian, and others. 2020. The stoichiometry of soil microbial biomass
599   determines metabolic quotient of nitrogen mineralization. Environ. Res. Lett. **15**: 034005.
600   doi:10.1088/1748-9326/ab6a26

601 Liu, S., T. Maavara, C. B. Brinkerhoff, and P. A. Raymond. 2022. Global Controls on DOC
602   Reaction Versus Export in Watersheds: A Damköhler Number Analysis. Glob.
603   Biogeochem. Cycles **36**: e2021GB007278. doi:10.1029/2021GB007278

604 Logue, J. B., C. A. Stedmon, A. M. Kellerman, N. J. Nielsen, A. F. Andersson, H. Laudon, E. S.
605   Lindström, and E. S. Kritzberg. 2016. Experimental insights into the importance of
606   aquatic bacterial community composition to the degradation of dissolved organic matter.
607   ISME J. **10**: 533–545. doi:10.1038/ismej.2015.131

608 Martí, E., N. B. Grimm, and S. G. Fisher. 1997. Pre- and Post-Flood Retention Efficiency of
609   Nitrogen in a Sonoran Desert Stream. J. North Am. Benthol. Soc. **16**: 805–819.
610   doi:10.2307/1468173

611 Mulholland, P. J., and W. R. Hill. 1997. Seasonal patterns in streamwater nutrient and dissolved
612   organic carbon concentrations: Separating catchment flow path and in-stream effects.
613   Water Resour. Res. **33**: 1297–1306. doi:10.1029/97wr00490

614 Natural Resources Conservation Service. Web Soil Survey. U. S. Dep. Agric.

615 Navel, S., F. Mermillod-Blondin, B. Montuelle, E. Chauvet, L. Simon, and P. Marmonier. 2011.
616   Water-Sediment Exchanges Control Microbial Processes Associated with Leaf Litter
617   Degradation in the Hyporheic Zone: A Microcosm Study. Microb. Ecol. **61**: 968–979.
618   doi:10.1007/s00248-010-9774-7

619 Niyogi, D. K., K. S. Simon, and C. R. Townsend. 2004. Land use and stream ecosystem
620   functioning: nutrient uptake in streams that contrast in agricultural development. Arch.
621   Für Hydrobiol. **160**: 471–486. doi:10.1127/0003-9136/2004/0160-0471

622 Ocampo, C., Oldham, C., and Sivapalan, M. 2020. Nitrate attenuation in agricultural catchments:
623   Shifting balances between transport and reaction - Ocampo - 2006 - Water Resources
624   Research - Wiley Online Library.

625 Oldham, C. E., D. E. Farrow, and S. Peiffer. 2013. A generalized Damköhler number for
626   classifying material processing in hydrological systems. Hydrol. Earth Syst. Sci. **17**:
627   1133–1148. doi:10.5194/hess-17-1133-2013

Perkins, D. M., G. Yvon-Durocher, B. O. L. Demars, J. Reiss, D. E. Pichler, N. Friberg, M. Trimmer, and G. Woodward. 2012. Consistent temperature dependence of respiration across ecosystems contrasting in thermal history. Glob. Change Biol. **18**: 1300–1311. doi:10.1111/j.1365-2486.2011.02597.x

Pinay, G., S. Peiffer, J.-R. De Dreuzy, and others. 2015. Upscaling Nitrogen Removal Capacity from Local Hotspots to Low Stream Orders' Drainage Basins. Ecosystems **18**: 1101–1120. doi:10.1007/s10021-015-9878-5

Ries III, K. G., J. K. Newson, M. J. Smith, and others. 2017. StreamStats, version 4.

Ryan, R. J., A. I. Packman, and S. S. Kilham. 2007. Relating phosphorus uptake to changes in transient storage and streambed sediment characteristics in headwater tributaries of Valley Creek, an urbanizing watershed. J. Hydrol. **336**: 444–457. doi:10.1016/j.jhydrol.2007.01.021

Schmid, B. H., I. Innocenti, and U. Sanfilippo. 2010. Characterizing solute transport with transient storage across a range of flow rates: The evidence of repeated tracer experiments in Austrian and Italian streams. Adv. Water Resour. **33**: 1340–1346. doi:10.1016/j.advwatres.2010.06.001

Sheibley, R. W., J. H. Duff, and A. J. Tesoriero. 2014. Low Transient Storage and Uptake Efficiencies in Seven Agricultural Streams: Implications for Nutrient Demand. J. Environ. Qual. **43**: 1980–1990. doi:10.2134/jeq2014.01.0034

Smith, R. A., R. B. Alexander, and G. E. Schwarz. 2003. Natural background concentrations of nutrients in streams and rivers of the conterminous United States. Environ. Sci. Technol. **37**: 3039–3047. doi:10.1021/es020663b

Thomas, S. A., H. Maurice Valett, J. R. Webster, and P. J. Mulholland. 2003. A regression approach to estimating reactive solute uptake in advective and transient storage zones of stream ecosystems. Adv. Water Resour. **26**: 965–976. doi:10.1016/S0309-1708(03)00083-6

Tromboni, F., S. A. Thomas, B. Gücker, and others. 2018. Nutrient Limitation and the Stoichiometry of Nutrient Uptake in a Tropical Rain Forest Stream. J. Geophys. Res. Biogeosciences **123**: 2154–2167. doi:10.1029/2018JG004538

Valett, H. M., J. A. Morrice, C. N. Dahm, and M. E. Campana. 1996. Parent lithology, surface-groundwater exchange, and nitrate retention in headwater streams. Limnol. Oceanogr. **41**: 333–345. doi:10.4319/lo.1996.41.2.0333

Vrugt, J. A., C. J. F. Ter Braak, C. G. H. Diks, B. A. Robinson, J. M. Hyman, and D. Higdon. 2009. Accelerating Markov Chain Monte Carlo Simulation by Differential Evolution with Self-Adaptive Randomized Subspace Sampling. Int. J. Nonlinear Sci. Numer. Simul. **10**. doi:10.1515/IJNSNS.2009.10.3.273

Wagner, K., M. M. Bengtsson, R. H. Findlay, T. J. Battin, and A. J. Ulseth. 2017. High light intensity mediates a shift from allochthonous to autochthonous carbon use in phototrophic stream biofilms. J. Geophys. Res. Biogeosciences **122**: 1806–1820. doi:10.1002/2016JG003727

Ward, A. S., and A. I. Packman. 2019. Advancing our predictive understanding of river corridor exchange. Wiley Interdiscip. Rev. Water **6**: e1327. doi:10.1002/wat2.1327

Ward, A. S., R. A. Payn, M. N. Gooseff, B. L. McGlynn, K. E. Bencala, C. A. Kelleher, S. M. Wondzell, and T. Wagener. 2013. Variations in surface water-ground water interactions along a headwater mountain stream: Comparisons between transient storage and water balance analyses. Water Resour. Res. **49**: 3359–3374. doi:10.1002/wrcr.20148

674 Webster, J. R., P. J. Mulholland, J. L. Tank, and others. 2003. Factors affecting ammonium
675   uptake in streams - an inter-biome perspective. Freshw. Biol. **48**: 1329–1352.
676   doi:10.1046/j.1365-2427.2003.01094.x

677 Wen, H., and L. Li. 2018. An upscaled rate law for mineral dissolution in heterogeneous media:
678   The role of time and length scales. Geochim. Cosmochim. Acta **235**: 1–20.
679   doi:10.1016/j.gca.2018.04.024

680 Wilhelm, L., K. Besemer, L. Fragner, H. Peter, W. Weckwerth, and T. J. Battin. 2015.
681   Altitudinal patterns of diversity and functional traits of metabolically active
682   microorganisms in stream biofilms. ISME J. **9**: 2454–2464. doi:10.1038/ismej.2015.56

683 Wondzell, S. M. 2006. Effect of morphology and discharge on hyporheic exchange flows in two
684   small streams in the Cascade Mountains of Oregon, USA. Hydrol. Process. **20**: 267–287.
685   doi:10.1002/hyp.5902

686 Zarnetske, J. P., M. N. Gooseff, T. R. Brosten, J. H. Bradford, J. P. McNamara, and W. B.
687   Bowden. 2007. Transient storage as a function of geomorphology, discharge, and
688   permafrost active layer conditions in Arctic tundra streams. Water Resour. Res. **43**: 7410.
689   doi:10.1029/2005WR004816

690 Zarnetske, J. P., R. Haggerty, S. M. Wondzell, V. A. Bokil, and R. González-Pinzón. 2012.
691   Coupled transport and reaction kinetics control the nitrate source-sink function of
692   hyporheic zones. Water Resour. Res. **48**. doi:10.1029/2012wr011894

693